Proton Nuclear Overhauser Effect Study of the Structure of a Deoxyoligonucleotide Duplex in Aqueous Solution†

David G. Reid, Stephen A. Salisbury, Sharon Bellard, Zippora Shakked,‡ and Dudley H. Williams*

ABSTRACT: Nuclear Overhauser enhancements (NOEs) have been observed between some of the nonexchangeable protons of the self-complementary octanucleoside heptaphosphate d(G-G-T-A-T-A-C-C) in conditions under which duplex formation takes place. Comparison of inter- and intraresidue NOEs has made possible the assignment of all the aromatic and 1′- and 2′-ribosyl signals. In particular, and with the exception of the 5′ terminal, NOEs of comparable magnitude are observed between H-8 of purines or H-6 of pyrimidines and pairs of anomeric protons. There are the H-1′s of the nucleotide containing the relevant aromatic proton and those of the adjacent residue in the 5′ direction. Differentially evolving NOEs are also generated between aromatic protons and the C-2′ methylene protons on both the same residue and on the neighboring 5′ residue. The relative magnitudes of these NOEs are discussed in terms of overall helical geometry and are consistent with a generally accepted B-type DNA model (R. Chandrasekaran and S. Arnott, personal communication).

The size of DNA and RNA polymers is such that given the limited resolving power of present techniques, detailed structural information cannot be obtained. Short fragments of DNA and RNA are potentially a source of the desired detailed structural information. The comparatively recent availability of synthetic deoxyoligonucleotides has made feasible this approach to studying DNA structure.

X-ray crystal analyses of a number of self-complementary sequences of up to 12 nucleotides have shown, in addition to the familiar A (Shakked et al., 1981) and B (Wing et al., 1980) geometries, some novel and unexpected features. The most striking of these are the left-handed double helix of Z-type DNA (Wang et al., 1979; Drew et al., 1980) and the concept of variation of the sugar–phosphate backbone to accommodate maximum base-stacking interactions (Viswamitra et al., 1978). These features have been correlated with polymer properties which were previously unexplained or unnoticed. Oligonucleotides, therefore, can be valid models capable of revealing details of polymer structure and may be particularly useful in discovering whether natural DNA contains conformationally characteristic regions.

Conformational determination in solution is more generally applicable and allows independent variation of the nature of oligomer and environment. It may also represent physiological conditions more closely. Proton NMR spectroscopy is the most powerful applicable solution method. It does not, however, give sufficiently precise or reliable information using the conventional parameters of chemical shift and coupling constants to define convincingly three-dimensional structure in molecules of this type. Recently, the nuclear Overhauser effect (NOE), a manifestation of through space dipolar relaxation (Noggle & Schirmer, 1971), has been applied successfully to obtain both qualitative information and quantitative information about the distances between protons in other large molecules (Tropp & Redfield, 1981; Alma et al., 1981; Williamson & Williams, 1981). We have been able to devise conditions which enable time-dependent NOEs to be observed between protons which are close (<4 Å), whether within a single nucleoside residue or between adjacent residues in the oligomer. This technique has made possible the assignment of the major part of the proton NMR spectrum of the octanucleoside heptaphosphate d(G-G-T-A-T-A-C-C). By comparison of the data with interproton distances calculated for standard structures, it has been possible to make deductions about the conformation of its duplex structure in solution. This structure may be contrasted with that in the crystal, which has already been determined (Shakked et al., 1981), and which displays an A-type geometry.

Materials and Methods

Nucleotides. The octamer d(G-G-T-A-T-A-C-C) was prepared by the solution triester method (Stawinski et al., 1977) and was purified by DEAE-cellulose column chromatography followed by reversed-phase (spherisorb ODS) high-pressure liquid chromatography. It was desalted by gel filtration (Sephadex G-25) and converted to its ammonium salt by passage through a column of ammonium Dowex AG 50-X8.

NMR Spectroscopy. All NMR spectra were obtained on a Bruker WH-400 operating in the Fourier transform mode. NOE difference spectra were obtained by alternately acquiring off-resonance and on-resonance irradiated spectra to minimize the effects of spectrometer drift. The decoupler power used was 18 dB, and 100 scans were accumulated for any one irradiation frequency. A delay time of 3 s was inserted between each accumulation to allow the system to reattain a steady state. The time dependence of the NOE was monitored by varying the irradiation time over the range 100–500 ms. A short delay of 2 ms was inserted between termination of irradiation and acquisition. The off-resonance irradiated (or control) spectrum was subtracted from the on-resonance spectrum to yield a NOE difference spectrum. NOE magnitudes were obtained by dividing the intensity of the observed peak by the intensity of the irradiated peak, both quantities being measured from difference spectra. The absolute values of NOEs from the thymine methyl protons are judged accurate to within 1%, while all other NOEs are probably accurate to within 3%. However, NOEs resulting from irradiation of the same proton can be compared to within an accuracy of about 2%.

Nucleotide Concentration. Three milligrams of nucleotide was dissolved in 0.4 mL of 99.98% enriched D_2O (Sigma) which was 100 mM in NaCl and 50 mM in phosphate ions, and gave a pH meter reading of 7.0. A trace of sodium 4,4-dimethyl-4-silapentanesulfonate (DSS) was added as an internal reference.

† From the University Chemical Laboratory, Cambridge, CB2 1EW, U.K. *Received February 9, 1982; revised manuscript received January 5, 1983.* This work was supported by the Science and Engineering Research Council and the Medical Research Council (U.K.).

‡ Present address: Department of Structural Chemistry, The Weizmann Institute of Science, Rehovot, Israel.

0006-2960/83/0422-2019$01.50/0

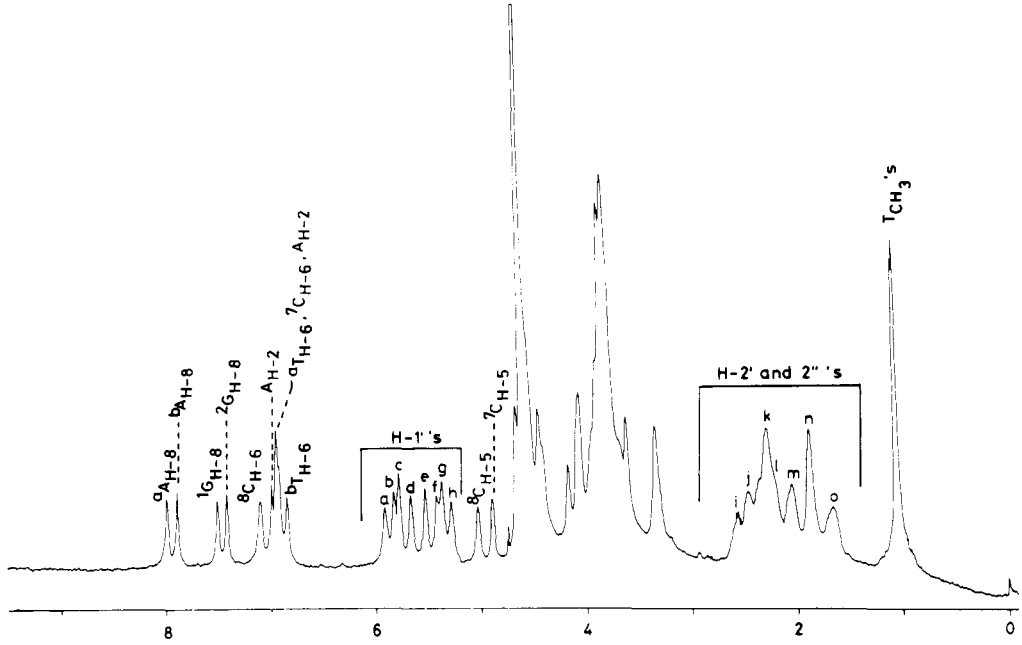

FIGURE 1: 400-MHz ^1H NMR spectrum of 3 mg of d(G-G-T-A-T-A-C-C) in 0.4 mL of ^2H_2O, 100 mM NaCl, and 50 mM phosphate at a pH meter reading of 7.0 and temperature of 10 °C. The nucleoside residues are numbered from the 5′ to the 3′ end. Where a resonance can be identified absolutely, it is named according to the number and type of its residue, e.g., $^8C_{H\text{-}5}$. Where the type but not the number of a residue can be identified, that resonance is distinguished by a superscript letter, e.g., $^aA_{H\text{-}8}$. Where only the type of resonance can be identified, single letters are used. No attempts to deal with the 3′, 4′, or 5′ signals has been made. The spectrum is the product of 100 accumulations.

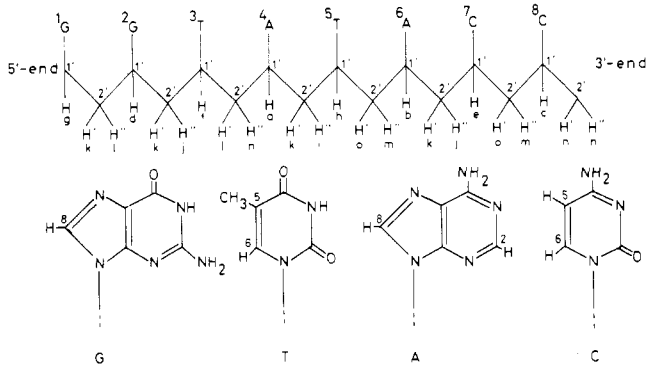

FIGURE 2: Schematic illustration of the octamer, summarizing the notation used and the eventual assignments.

Model Building. Kendrew wire models were used for model building. Interatomic distances for the A-type double helix (Arnott & Hukins, 1972) were calculated after hydrogen atoms were generated in geometrically reasonable positions with a C–H bond length of 1.08 Å. Coordinates of hydrogen atoms supplied by Dr. S. Arnott (R. Chandrasekaran and S. Arnott, personal communication) were used directly to calculate interproton distances in the B-type helix.

Results and Discussion

The ^1H NMR spectrum of the self-complementary octanucleoside heptaphosphate d(G-G-T-A-T-A-C-C) is shown in Figure 1. The numbering and lettering which is used in assigning the proton spectrum is summarized in Figure 2.

Spectral Assignment. The temperature dependence of the proton spectrum was monitored over the temperature range 0–80 °C. Cooling is accompanied by spectral changes usually assumed to result from increased base stacking as a Watson–Crick double helix is formed. The most important of these are upfield shifts of certain resonances, notably the cytidine H-5s and H-6s, whose chemical shifts are plotted against temperature in Figure 3, and the adenine H-2s. Of these resonances, the former two types are unique in displaying a doublet structure at higher temperatures, while the latter type shows a particularly long longitudinal relaxation time. Resolved splittings of the cytidine H-5s and H-6s (and also of H-1′s) cannot be seen at 10 °C (Figure 1) due to the relatively

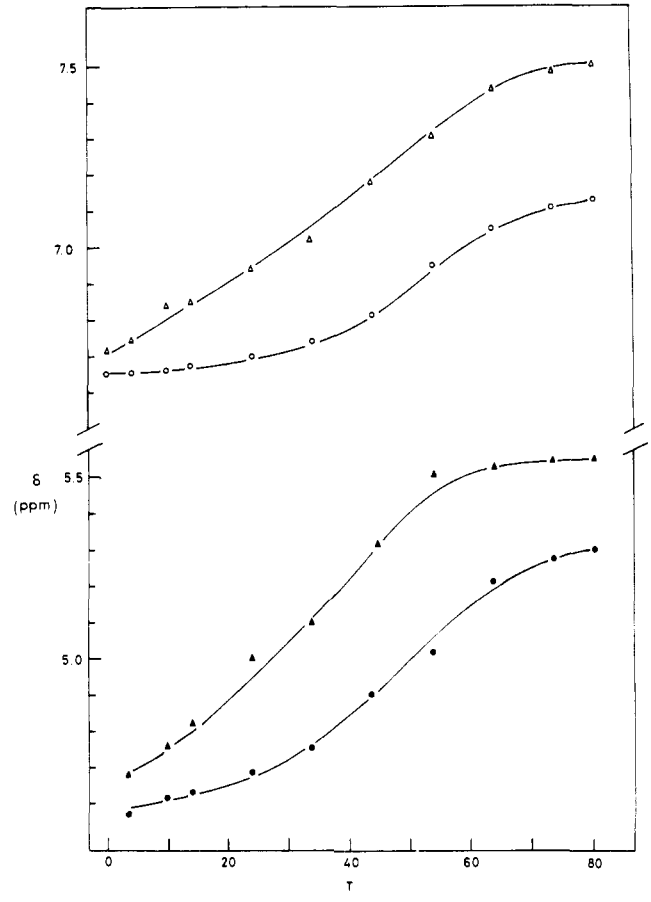

FIGURE 3: Temperature dependence of the cytidine ring proton chemical shifts measured in ppm downfield of internal DSS. (△) $^8C_{H\text{-}6}$, (○) $^7C_{H\text{-}6}$, (▲) $^8C_{H\text{-}5}$, and (●) $^7C_{H\text{-}5}$. Temperature is shown in °C.

Table I: Percentage NOEs in d(G-G-T-A-T-A-C-C)[a]

observed resonance	NOE (%) for irradiated resonance																
	$^{a}A_{H\text{-}8}$	$^{b}A_{H\text{-}8}$	$^{1}G_{H\text{-}8}$	$^{2}G_{H\text{-}8}$	$^{8}C_{H\text{-}6}$	$^{7}C_{H\text{-}6}$ and $^{a}T_{H\text{-}6}$	$^{b}T_{H\text{-}6}$	a	b, c	d	e	f	g	h	$^{8}C_{H\text{-}5}$	$^{7}C_{H\text{-}5}$	T_{CH_3}
$^{a}A_{H\text{-}8}$								6				4					3
$^{b}A_{H\text{-}8}$									4					7			
$^{1}G_{H\text{-}8}$													4				
$^{2}G_{H\text{-}8}$										6			5				3
$^{8}C_{H\text{-}6}$									6		7				21		
$^{7}C_{H\text{-}6}$, $^{a}T_{H\text{-}6}$									7	11	8	10				23	5
$^{b}T_{H\text{-}6}$								5						7			3
a	12						8										3
b		12				4										5	
c					10												
d				10		5											2
e					8	3									4		
f	11					5											
g			11	15													
h		9					15										
$^{8}C_{H\text{-}5}$					26	3					3						
$^{7}C_{H\text{-}5}$		7				10			2								
i	*7*						*10*	*15*									*2*
j		*8*		*16*		*7*			*8*	*9*						6	*2*
k		*16*	*17*				*5*	*10*	*3*	*6*			*10*			5	*4*
l	*24*		*11*	*33*		*9*						*7*	*18*				
m		*7*			*6*	*4*	*10*				*16*			*16*	*7*		
n	*6*				*14*	*9*			*18*			*13*					
o		*6*			*7*	*8*	*23*				*9*			*8*	6		
T_{CH_3}s	25			26		10	49	6		9							

[a] All NOEs were measured after an irradiation time of 0.5 s, except those from the aromatic (excluding the cytidine H-5s) and anomeric signals to the 2′-methylenes. These NOEs evolved rapidly and were measured after 0.2-s irradiation, and they are distinguished by italicized numbers. Positive numbers represent negative NOEs.

long correlation time for molecular tumbling at this temperature. The cytidine H-6s (and H-5s) may be distinguished by their relative chemical shifts. The higher field signals may be assigned to the internal cytidine ring (i.e., ^{7}C) as they experience the strong ring-current shielding of both an adenine ring and a cytosine ring, while the lower field signals are shielded by only a cytosine ring and must thus be assigned to ^{8}C. The guanine H-8s may be distinguished from the adenine H-8s by the former's property of exchanging more rapidly with solvent deuterium. Chemical shift arguments of a qualitative nature similar to those used for the cytidine protons suggest that the lower field guanine H-8 may be ascribed to the terminal guanosyl (i.e., ^{1}G) and the higher field signal to ^{2}G. No such ready distinction is possible among the adenosyl and thymidylyl aromatic signals.

Assignment of the eight distinct H-1′ resonances is impossible on the basis of chemical shift arguments, although they are well resolved at 10 °C. The 16 expected chemically distinct 2′-methylene signals overlap considerably, and once again chemical shifts are of no help in assignment. Thus, in an oligonucleotide of this size, conventional assignment techniques appear to be limited to aromatic protons, and distinctions even between them are not necessarily straightforward.

Nuclear Overhauser Effect Measurements. A temperature of 10 °C was chosen as optimal for NOE measurements for the following reasons. Above this temperature considerable melting of the ends of the helix has taken place, as is evident from the downfield shifts of $^{8}C_{H\text{-}5}$ and $^{8}C_{H\text{-}6}$. Below 10 °C signal broadening becomes excessive.

Spin diffusion in a slowly tumbling macromolecule can be considerable and renders the conventional steady-state Overhauser effect of little use in the measurement of internuclear distances (Kalk & Berendsen, 1976). These distances may be derived, however, from an experiment in which a particular resonance is saturated for a time τ, which is short relative to the longitudinal relaxation times of neighboring nuclei, and NOEs measured immediately subsequent to the termination of the saturating pulse (Wagner & Wüthrich, 1979). The process may be repeated for an enhanced S/N ratio if a suitable delay of about 4 times the spin–lattice relaxation time of the observed nuclei is inserted between the saturation–accumulation sequence. If, in addition, a series of experiments is performed in which the saturation time is varied before accumulation of the free induction decay, the rate at which saturation is transferred to neighboring nuclei may be measured. This rate is a function of internuclear distances, and by use of a short saturating pulse those nuclei closest to the irradiated proton may be distinguished from those lying at a greater distance.

NOEs observed in the octanucleotide at 10 °C are negative and are displayed in Table I. Build up of the NOE was measured by using saturation times of 0.1, 0.2, 0.35, and 0.5 s, but only the percentage saturation transfers for some of these times are shown. Some representative NOE difference spectra are illustrated in Figure 4. Irradiation of $^{a}A_{H\text{-}8}$ causes an NOE to build up rapidly to the 2′-proton signals i and k (and rather more slowly to l and n). Also observed are more slowly evolving effects to the anomeric protons a and f and to the thymine methyl resonances. Similar irradiation at the thymine methyl signal produces NOEs to the 2′ signals i, j, and k, the anomeric resonances a and d, the two $T_{H\text{-}6}$s, $^{a}A_{H\text{-}8}$, and $^{2}G_{H\text{-}8}$. NOEs resulting from irradiations at all the aromatic and anomeric signals are shown in Table I.

Interpretation of the observed NOEs requires that some basic assumption regarding the conformation of the duplex must be made; our initial working assumption is that it adopts a right-handed helical structure. It is also important to establish that the longitudinal relaxation is dominated by interproton dipolar interactions and furthermore that the motion modulating this relaxation is isotropic. Early et al. (1980) have

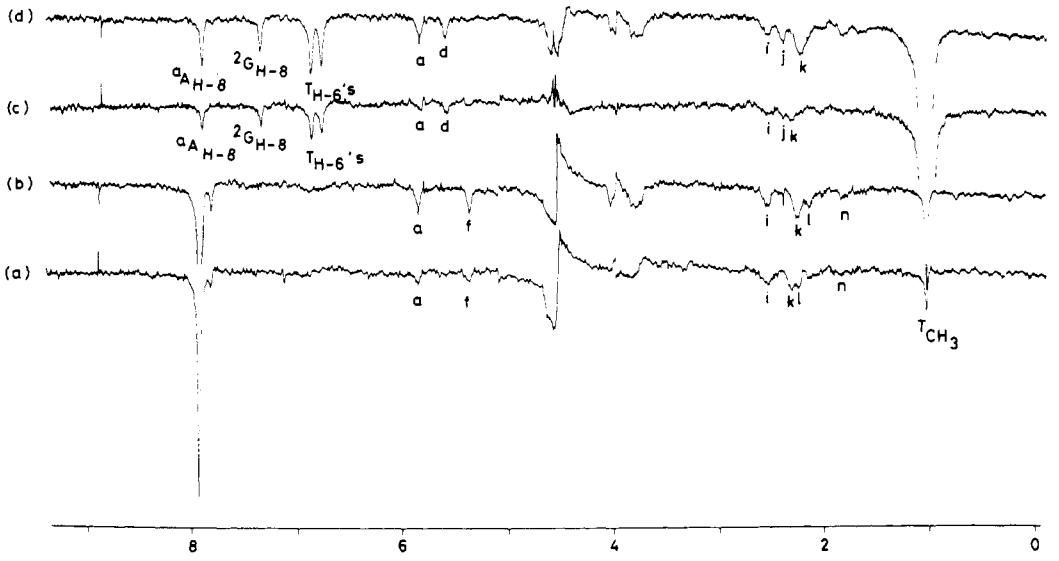

FIGURE 4: NOE difference spectra for the irradiation of $^{a}A_{H-8}$ and the thymine methyls. (a) and (b) show the results of 0.2- and 0.5-s irradiations, respectively, of $^{a}A_{H-8}$, while (c) and (d) result from 0.2- and 0.5-s irradiations, respectively, of the thymine methyls.

studied a 12 base pair restriction fragment and have found both conditions to be met. When the dimensions of the duplex under study here are considered, it seems unlikely that NOEs will be complicated by anisotropic tumbling. In highly asymmetric molecules, however, such as sheared natural or synthetic DNA in which the rate of rotation about the helix axis may be expected to exceed the rate of end-over-end tumbling by a large amount, the effect of this anisotropic motion on NOEs must be taken into account. Molecular model building provides some initial rationalization of the NOEs. It is apparent that certain protons or groups of protons are close to each other regardless of precise helical geometry. This may be seen, for example, from the data given in Table III, to which we will make more detailed reference subsequently. For instance, a purinyl H-8 appears to be close to the 5-substituent on a pyrimidine ring adjacent to it in the 3′ direction. This observation immediately explains the NOE from $^{a}A_{H-8}$ to the thymine methyls and furthermore allows $^{a}A_{H-8}$ to be assigned as $^{4}A_{H-8}$; $^{6}A_{H-8}$ is adjacent to a cytidine in the 3′ direction. Also explained are the NOEs from the methyl groups to $^{a}A_{H-8}$ (from $^{5}T_{CH_3}$) and to $^{2}G_{H-8}$ (from $^{3}T_{CH_3}$). Similarly, a purinyl H-8 is approximately the same distance from the H-1′ on its own nucleoside residue, as from the anomeric proton on the next residue in the 5′ direction. Thus signals a and f (Table I and Figure 2) must be $^{4}A_{H-1'}$ and $^{3}T_{H-1'}$ (not necessarily respectively). When it is noted that in certain conformers the pyrimidine 5-substituent is close to the H-1′ proton of the adjacent residue in the 5′ direction, the NOEs to the anomeric protons a and d (Table I and Figure 2), observed when the methyls are irradiated, may be rationalized. These resonances must correspond to $^{4}A_{H-1'}$ and $^{2}G_{H-1'}$. Since a is also perturbed when $^{4}A_{H-8}$ is irradiated, it is assigned as $^{4}A_{H-1'}$, and d is $^{2}G_{H-1'}$. Thus f, also perturbed by saturation of $^{4}A_{H-8}$, is $^{3}T_{H-1'}$.

In an analogous way, the NOEs resulting from irradiation of all the aromatic signals may be used to assign the anomeric resonances. For instance, irradiation of $^{6}A_{H-8}$ causes NOEs to the anomeric protons b and h, as well as to $^{7}C_{H-5}$. Saturation of $^{7}C_{H-5}$ causes an NOE to b, and when these facts are considered together, b must be $^{6}A_{H-1'}$ and h, $^{5}T_{H-1'}$. Irradiation of $^{1}G_{H-8}$ produces an NOE to only a single H-1′ proton, as would be expected from the absence of a residue adjacent to it in the 5′ direction. Thus, g is $^{1}G_{H-1'}$. This fact and the NOEs to d and g when $^{2}G_{H-8}$ is irradiated allow us to identify the former with $^{2}G_{H-1'}$. NOEs are seen from $^{8}C_{H-6}$ to c and e and from the signal corresponding to overlap of $^{7}C_{H-6}$ and $^{a}T_{H-6}$ to the four H-1′ resonances b, d, e, and f. Thus e may be assigned as $^{7}C_{H-1'}$, and therefore c must be $^{8}C_{H-1'}$. Since b and d have already been identified, f can only correspond to $^{a}T_{H-1'}$. As the NOE to $^{2}G_{H-1'}$ (i.e., d) can arise only from $^{3}T_{H-6}$, this must correspond to $^{3}T_{H-6}$, and f to $^{3}T_{H-1'}$. The NOEs from $^{b}T_{H-6}$, now identifiable as $^{5}T_{H-6}$, serve to confirm assignments of a and h as $^{4}A_{H-1'}$ and $^{5}T_{H-1'}$, respectively.

Having assigned the H-1′ protons by irradiation of the aromatic proton resonances, it may be seen that when the H-1′ signals are irradiated in their turn, the NOEs to the aromatic proton resonances are consistent with the prior assignments. Knowledge of the H-1′ assignments is particularly useful in analyzing the 2′ region of the spectrum. The distances between H-1′ and the 2′-methylene protons on the same ribose ring are only slightly dependent on the ring geometry. A 2′-endo conformation places H-1′ 3.1 Å from H-2′ (the methylene proton "trans" to it) and 2.6 Å from H-2″ ("cis" to H-1′). If the ring is allowed to adopt a 3′-endo pucker, the distance to H-2″ remains substantially the same, while H-2′ approaches to 2.7 Å. In no reasonable right-handed helical form does any H-1′ approach closer than 4.0 Å to a 2′ proton on any other ribosyl residue. Thus NOEs from H-1′ signals should identify the vicinal methylene pair exclusively, and their relative buildup rates should make distinction between the two geminal methylene protons possible.

Indeed when a (i.e., $^{4}A_{H-1'}$) is irradiated, differentially evolving NOEs are observed to the 2′ signals i and k, in that order of magnitude, suggesting that i is due to $^{4}A_{H-2''}$ and k to $^{4}A_{H-2'}$. Separate irradiation of b and c is difficult, but when they are saturated simultaneously, a strong NOE is seen to n, and weaker NOEs to j and k. In this way it is possible to ascribe each methylene proton to a signal in the high-field region of the spectrum. The observation of only three NOEs when b and c are irradiated is explained if two simultaneously perturbed resonances are coincident. All the NOEs discussed thus far are consistent with the assignments shown in Table II.

Having assigned the 2′-methylene region of the spectrum, it should be possible to rationalize the NOEs to these protons from the aromatic region. It is immediately apparent that the situation is complicated by intraresidue effects. In an attempt to resolve these complications, it was necessary to refine the

Table II: Assignment of the ^{1}H NMR Spectrum of d(G-G-T-A-T-A-C-C) Made Possible by NOEs

code	assignment	code	assignment
^{a}A$_{H-8}$	^{4}A$_{H-8}$	g	^{1}G$_{H-1'}$
^{b}A$_{H-8}$	^{6}A$_{H-8}$	h	^{5}T$_{H-1'}$
^{a}T$_{H-8}$	^{3}T$_{H-6}$	i	^{4}A$_{H-2''}$
^{b}T$_{H-6}$	^{5}T$_{H-6}$	j	^{6}A$_{H-2''}$, ^{2}G$_{H-2''}$
a	^{4}A$_{H-1'}$	k	^{4}A$_{H-2'}$, ^{6}A$_{H-2'}$
b	^{6}A$_{H-1'}$		^{1}G$_{H-2'}$, ^{2}G$_{H-2'}$
c	^{8}C$_{H-1'}$	l	^{1}G$_{H-2''}$, ^{3}T$_{H-2'}$
d	^{2}G$_{H-1'}$	m	^{5}T$_{H-2''}$, ^{7}C$_{H-2''}$
e	^{7}C$_{H-1'}$	n	^{8}C$_{H-2''}$, ^{3}T$_{H-2''}$, ^{8}C$_{H-2'}$
f	^{3}T$_{H-1'}$	o	^{5}T$_{H-2'}$, ^{7}C$_{H-2'}$

Table III: Relevant Short Interproton Distances in Models of Two DNA Conformations

type of interproton vector	interproton distances (Å)			
	intraresidue		interresidue[a]	
	B form	A form	B form	A form
H-8···H-1′	3.8	3.8	3.6	4.0
H-6···H-1′	3.7	3.6	3.5	4.0
H-5···H-1′	>5.0	>5.0	4.3	4.8
H-5···H-5			4.7	3.8
H-5···H-6	2.5	2.5	3.9	>5.0
H-5···H-8			3.9	3.8
H-8···H-2′	2.3	3.9	3.9	1.7
H-8···H-2″	3.5	4.7	2.1	3.3
H-6···H-2′	2.0	3.8	4.0	1.6
H-6···H-2″	3.3	4.4	2.2	3.1
H-5···H-2′	4.3	>5.0	3.5	3.0
H-5···H-2″	>5.0	>5.0	3.0	4.8
T_{CH_3}···H-8[b]			3.3	3.1
T_{CH_3}···H-1′	>5.0	>5.0	3.8	4.8
T_{CH_3}···H-2′	4.8	>5.0	2.9	2.8
T_{CH_3}···H-2″	>5.0	>5.0	2.6	4.5
T_{CH_3}···H-6	2.7	2.8		
H-1′···H-2′	3.1	2.7	4.6	4.6
H-1′···H-2″	2.6	2.3	>5.0	>5.0
H-2′···H-2″	1.8	1.8	>5.0	>5.0

[a] The first proton in the left-hand column is assumed to be in the residue adjacent in the 3′ direction to the residue containing the second proton. Thus the vector H-8···H-1′ would correspond to the distance between ^{2}G$_{H-8}$ and ^{1}G$_{H-1'}$. [b] Distances involving methyl groups are means, calculated by measuring the lengths of the three vectors from each methyl proton to the other proton concerned, the methyl being held in a suitable staggered conformation. The mean is calculated by using the formula $r = [1/3(1/r_1^6 + 1/r_2^6 + 1/r_3^6)]^{-1/6}$.

models on which our assignments hitherto had been based. The intranucleotide H···H contacts between aromatic and ribose protons depend on the sugar geometry and the orientation of the base with respect to the sugar, whereas the internucleotide contacts depend also on the helical parameters. Coordinates of uniform model A- (Arnott & Hukins, 1972) and B-DNA (R. Chandrasekaran and S. Arnott, personal communication) helices were used inserting protons where necessary in geometrically reasonable positions to calculate relevant H···H distances. Those less than 5 Å are shown in Table III. Some of the H···H contacts are too short (1.6–1.9 Å) in the A-DNA model and result from the assumption of a rigid uniform geometry and failure to consider hydrogen atoms. In flexible oligonucleotides these distances may be increased to values in the range 2.0–2.5 Å. We have assumed the distances of Table III to represent approximate interproton contacts in the two DNA forms.

Although the H-1′ resonances are well resolved, their line widths preclude any observation of coupling constants. Moreover the observation of both 2′-*endo*- and 3′-*endo*-furanose conformers in two crystal structures of oligonucleotides, one displaying an alternating B-DNA conformation (Klug et al., 1979) and the other a modified A-DNA structure (Wang et al., 1982), shows that sugar pucker is not necessarily a reliable index of overall DNA geometry. We believe that NOEs, which can probe relationships between the residues in the double helix, provide a potentially far better basis for this distinction than do either chemical shifts or individual ribose conformations. It will be noticed that in a B-type conformation, the H-8 of a purine or the H-6 of a pyrimidine is in close proximity both to the H-2′ on its own nucleotide residue (2.3 and 2.0 Å in the case of a purine or pyrimidine, respectively) and to the H-2″ associated with the residue adjacent to it in the 5′ direction (2.1 and 2.2 Å). The same aromatic proton is rather further away from the H-2″ of its own residue (3.5 and 3.3 Å for a purine or pyrimidine nucleotide, respectively) and from the H-2′ of the next 5′ residue (3.9 and 4.0 Å). The order of these distances is significantly different in the model A-form helix. Both H-8 of a purine and H-6 of a pyrimidine are rather remote from their own H-2′ and H-2″ protons (3.9 and 4.7 Å, respectively, in the case of the purine and 3.8 and 4.4 Å for a pyrimidine). However, when separations from the corresponding 2′ protons on the next residue in the 5′ direction are considered, they are seen to be much shorter: 1.7 and 3.3 Å from a purine H-8 to the H-2′ and H-2″s, and 1.6 and 3.1 Å from a pyrimidine H-6 to the same methylenes. A schematic illustration of the changes in geometry between A and B forms which might be probed by NOEs is given in Figure 5. The close interaction between H-2′ and H-6 (or H-8) on the adjacent base, in the 5′ direction in the A form, is absent in the B form. The changes in orientation and conformation of the furanose ring cause the generation of three new short distances (indicated by double-headed arrows in B of Figure 5). Thus, the pattern of NOEs observed when an H-8 or H-6 is irradiated might be expected to reflect the type of helix geometry adopted, and indeed this seems to be the case.

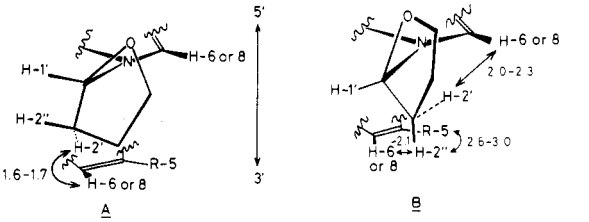

FIGURE 5: Schematic illustration showing changes in some close interactions between A and B forms of DNA.

When ^{a}A$_{H-8}$ (i.e., ^{4}A$_{H-8}$) is saturated, an NOE builds up rapidly to the group of resonances associated with k and l; the effect to the latter is obvious in the difference spectrum as a shoulder on the NOE to k, which is clearly the larger of the two. Also observed are NOEs to i and n whose evolution is rather less rapid. The H-1′ irradiations have already made possible the identification of i with ^{4}A$_{H-2''}$ and part of k with ^{4}A$_{H-2'}$, while ^{3}T$_{H-2'}$ and ^{3}T$_{H-2''}$ contribute to l and n. If the oligonucleotide exhibited a pure B-form geometry, NOEs would be expected to evolve rapidly to ^{4}A$_{H-2'}$ and ^{3}T$_{H-2''}$ (i.e., to k and n) with slower effects to ^{4}A$_{H-2''}$ and ^{3}T$_{H-2'}$ (i.e., i and l). The strongest influence does indeed seem to be to k, although the situation is complicated by the partial overlap of ^{4}A$_{H-2'}$ and ^{3}T$_{H-2'}$. The situation is rather clearer in the instance of ^{6}A$_{H-8}$ irradiation; a strong NOE is observed to k, with weaker effects of j, m, and o. Irradiation of b, i.e., ^{6}A$_{H-1'}$ (which overlaps ^{8}C$_{H-1'}$), has already suggested that portions of j and k might be ascribed to ^{6}A$_{H-2''}$ and ^{6}A$_{H-2'}$, respectively. ^{6}A$_{H-8}$ irradiation confirms that these signals are associated with

the ^{6}A residue (rather than with ^{8}C, a possibility remaining from the irradiation of b and c). The strongest NOE being to k (i.e., $^{6}A_{H\text{-}2'}$) is evidence of B geometry, although the buildup rates for the various effects are not quantitatively consistent with the distances in Table III. Considering the extreme proximity of $^{6}A_{H\text{-}8}$ to $^{5}T_{H\text{-}2'}$ (signal o) which is a consequence of an A-type geometry (see Figure 3), the relatively small NOE to this position seems to indicate a negligible or small (<10%) population of the A form, at least in this region of the duplex.

Irradiation of $^{1}G_{H\text{-}8}$ and $^{2}G_{H\text{-}8}$ is rendered relatively uninformative by the considerable overlap of the relevant 2′ protons. In the former case, NOEs are observed to k and l, consistent with contributions to these signals from $^{1}G_{H\text{-}2'}$ and $^{1}G_{H\text{-}2''}$, respectively. These protons also receive saturation transferred from $^{2}G_{H\text{-}8}$, as does $^{2}G_{H\text{-}2'}$ (also contributing to k) and $^{2}G_{H\text{-}2''}$ (signal j).

Saturation of $^{8}C_{H\text{-}6}$ results in a rapid NOE buildup to signal n (containing both ^{8}C 2′-methylene proton resonances) and smaller effects to signals m and o, which contain intensity from $^{7}C_{H\text{-}2''}$ and $^{7}C_{H\text{-}2'}$, respectively. Again there is evidence for little contribution from an A form based on the relative insignificance of the NOE to $^{7}C_{H\text{-}2'}$. Similarly, the strongest NOE observed from $^{b}T_{H\text{-}6}$ (i.e., $^{5}T_{H\text{-}6}$) is to signal o (containing $^{5}T_{H\text{-}2'}$). Next in order of magnitude are NOEs to i and m, which contain $^{4}A_{H\text{-}2''}$ and $^{5}T_{H\text{-}2''}$; the weakest NOE to the 2′ region is that seen to k ($^{4}A_{H\text{-}2'}$). NOEs resulting from irradiation of the signal containing $^{7}C_{H\text{-}6}$ and $^{3}T_{H\text{-}6}$ are complicated by overlap in the 2′ region but are generally consistent with a B geometry.

If the distances from the pyrimidine ring 5-substituents are considered, it will be noted that a B geometry places a cytidine H-5 3.5 and 3.0 Å, respectively, away from H-2′ and H-2″ on the adjacent 5′ residue, with a thymine methyl group on average 2.9 and 2.6 Å from the same protons (Table III). The corresponding lengths for the model A form are 3.0 and 4.8, and 2.8 and 4.5. Nearly equal NOEs are in fact observed when $^{8}C_{H\text{-}5}$ and $^{7}C_{H\text{-}5}$ are irradiated, to m ($^{7}C_{H\text{-}2''}$) and o ($^{7}C_{H\text{-}2'}$) and to j($^{6}A_{H\text{-}2''}$) and k ($^{6}A_{H\text{-}2'}$), respectively. Similarly thymine methyl irradiation results in NOEs to i ($^{4}A_{H\text{-}2''}$), j (containing $^{2}G_{H\text{-}2''}$), and k (containing $^{4}A_{H\text{-}2'}$ and $^{2}G_{H\text{-}2''}$). Considering the inverse sixth power dependence of the NOE on distance, the comparable sizes of the effects to the H-2′s and H-2″s are difficult to reconcile with the interproton separations in an A conformer.

It will be seen that in general the aromatic–anomeric internucleotide distances are of the same order as the corresponding intranucleotide distances in both the A-form and the B-form models. Thus the NOEs observed between these types of protons are of little utility in distinguishing between the two conformational families. However, the NOEs generated between the aromatic and C-2′ methylene protons do seem to be consistent with an overall B conformation. Any contribution to the observed structure resulting from a significant fraction of A form seems to be excluded on the grounds of the very short distance between H-8 or H-6 and the H-2′ proton of the adjacent residue, which would cause much larger NOEs to be observed between these protons than is actually the case.

It is important to appreciate that a portion of the logic used in the study (assumed approximate conformation → assignments based on NOEs → consideration of a refined conformation) does not lead to pitfalls which might be associated with a circular argument. The assignments are secure because of the use of additional information (such as J splitting and chemical shifts) and the demands made by the known sequence and in particular the nature of the terminal residues. For example, some of the aromatic protons of the G and C residues were assigned before the consideration of NOEs. It is then found that interresidue NOEs assigned as occurring at 3′ → 5′ direction are indeed absent for the (prior assigned) ^{1}G nucleotide unit.

NOEs are capable in principle of yielding absolute distances between nuclei in a rigid structure. Three factors in this study militate against deriving such distances. First, the flexibility of the helical structure implies that any distances derived would necessarily be time-average values. Second, such distance derivations require accurate measurement of NOE buildup rates after very short irradiation times. The very large line widths, especially of the crucial C-2′ methylenes, make such measurements extremely time consuming. Third, even a small amount of spin diffusion could seriously compromise quantitative results based on longer irradiation times.

Conclusion

Three important conclusions follow from this study. First, NOEs are extremely useful in assigning proton spectra of oligonucleotides without recourse to laborious incremental synthesis methods, or unreliable chemical shift arguments. Second, gross features of helix geometry may be deduced and may allow distinction between A- and B-form conformations. We are in the process of testing this assertion further in studies on hybrids between oligodeoxy- and oligoribonucleotides. Third, it is clear that intermolecular NOEs should prove invaluable in future studies of interactions between oligonucleotides and DNA-binding drugs and antibiotics.

Acknowledgments

We thank Graciela B. Sala for her valuable contribution to the synthetic work and Dr. O. Kennard for her interest in this study. D.G.R. acknowledges financial support from the C.S.I.R. (S.A.), D.G.R. and D.H.W. from S.E.R.C. (U.K.), and S.A.S. from M.R.C. (U.K.).

Registry No. d(G-G-T-A-T-A-C-C), 80407-93-8.

References

Alma, N. C. H., Harmsen, B. J. M., Hull, W. E., van der Marel, G., van Boom, J. H., & Hilbers, C. W. (1981) *Biochemistry 20*, 4419–4428.

Arnott, S., & Hukins, D. W. L. (1972) *Biochem. Biophys. Res. Commun. 47*, 1504–1509.

Drew, H., Tanaka, S., Itakura, K., & Dickerson, R. E. (1980) *Nature (London) 286*, 567–573.

Early, T. A., Kearns, D. R., Hillen, W., & Wells, R. D. (1980) *Nucleic Acids Res. 8*, 5795–5812.

Kalk, A., & Berendsen, H. J. C. (1976) *J. Magn. Reson. 24*, 343–366.

Klug, A., Jack, A., Viswamitra, A., Kennard, O., Shakked, Z., & Steitz, T. A. (1979) *J. Mol. Biol. 131*, 669.

Noggle, J. H., & Schirmer, R. E. (1971) *The Nuclear Overhauser Effect: Chemical Applications*, Academic Press, New York.

Shakked, Z., Rabinovich, D., Cruse, W. B. T., Egert, E., Kennard, O., Sala, G., Salisbury, S. A., & Viswamitra, M. A. (1981) *Proc. R. Soc. London, Ser. B B213*, 479–482.

Stawinski, J., Hozumi, T., Narang, S. A., Bahl, C. P., & Wu, R. (1977) *Nucleic Acids Res. 4*, 353–371.

Tropp, J., & Redfield, A. G. (1981) *Biochemistry 20*, 2133–2140.

Viswamitra, M. A., Kennard, O., Jones, P. G., Sheldrick, G. M., Salisbury, S., Falvello, L., & Shakked, Z. (1978) *Nature (London) 273*, 687–688.

Wagner, G., & Wüthrich, K. (1979) *J. Magn. Reson. 33*, 675–680.
Wang, A. H.-J., van Boom, J. H., van der Marel, G., Rich, A., Quigley, G. J., & Kolpack, F. J. (1979) *Nature (London) 282*, 680–686.
Wang, A. H.-J., Fujii, S., van Boom, J. H., & Rich, A. (1982) *Proc. Natl. Acad. Sci. U.S.A. 79*, 3968–3972.
Williamson, M. P., & Williams, D. H. (1981) *J. Am. Chem. Soc. 103*, 6580.
Wing, R., Drew, H., Takano, T., Broka, C., Tanaka, S., Itakura, K., & Dickerson, R. E. (1980) *Nature (London) 287*, 755–758.

Topoisomerase I from Chicken Erythrocytes: Purification, Characterization, and Detection by a Deoxyribonucleic Acid Binding Assay†

James V. Tricoli‡ and David Kowalski*

ABSTRACT: We have purified a deoxyribonucleic acid topoisomerase to near homogeneity from the nuclei of mature chicken erythrocytes. The enzyme relaxes supercoiled DNA in the absence of ATP or Mg^{2+}. It is unable to resolve topologically knotted circular duplex DNA. These properties resemble those of type I eukaryotic topoisomerases capable of breaking and rejoining one strand of duplex DNA at a time. The sedimentation value of the protein is 4.4 S. The molecular weight of the reduced, denatured protein is 100K. After elution from sodium dodecyl sulfate ($NaDodSO_4$) gels and renaturation, topoisomerase activity is found in the band at 100K and in minor bands at 95K, 78K, and 73K. The minor bands are likely to be proteolytic fragments since the M_r 100K protein is cleaved by trypsin to fragments of similar or even smaller size with retention of activity. At KCl concentrations suboptimal for the 100K form, the trypsin cleaved form is severalfold more active than the 100K form. Single-stranded DNA, but not duplex DNA or RNA, inhibits DNA relaxing activity, presumably by forming a covalent complex at the enzyme active site. Preincubation of the enzyme with single-stranded DNA leads to the depletion, in $NaDodSO_4$–polyacrylamide gels, of protein bands corresponding to the 100K topoisomerase, its putative proteolytic fragments, and its tryptic fragments. The reaction which leads to band depletion requires active topoisomerase and conditions where single-stranded DNA inhibits relaxing activity. The band depletion technique provides a convenient assay for the polynucleotide binding activity of topoisomerases and possibly other proteins. The function of the enzyme in the inactive nuclei of mature chicken erythrocytes is unclear. The estimated content of chicken erythrocyte topoisomerase per unit DNA is comparable to that in nuclei active in replication and transcription.

Topoisomerases are enzymes which can interconvert different topological isomers of circular duplex DNA by catalyzing the concerted breaking and rejoining of DNA backbone bonds [for reviews see Champoux (1978a,b), Gellert (1981), Wang & Liu (1979), and Cozzarelli (1980)]. Two types of topoisomerases can be formally distinguished by the mechanism of their breakage–reunion reaction (Liu et al., 1980). Type I topoisomerases act on one strand of duplex DNA at a time while type II enzymes act simultaneously on both strands. In eukaryotes, known type I enzymes do not require ATP (Champoux, 1978a,b; Gellert, 1981; Wang & Liu, 1979; Cozzarelli, 1980) while known type II enzymes do (Liu et al., 1980; Baldi et al., 1980; Hsieh & Brutlag, 1980). Additionally, the two types can be operationally distinguished by the ability of type II but not type I enzymes to produce or resolve catenated forms of covalently closed circular DNA and to remove knots from duplex DNA (Liu et al., 1980, 1981; Baldi et al., 1980; Hsieh & Brutlag, 1980; Mizuuchi et al., 1980; Kreuzer & Cozzarelli, 1980).

Historically, the major type I topoisomerase activity in eukaryotic cells was referred to as the DNA nicking–closing enzyme (also known as untwisting enzyme and relaxing enzyme). The enzyme relaxes supercoiled DNA in the absence of added cofactors and is found in nuclei. The enzyme has been highly purified from several sources (Keller, 1975; Champoux & McConaughy, 1976; Tang, 1978). The reduced, denatured protein consists of a single polypeptide chain of molecular weight (M_r)[1] 60 000–70 000 (60K–70K).

More recently, a type I enzyme designated topoisomerase I has been purified from HeLa cells (Liu & Miller, 1981), wheat germ (Dynan et al., 1981), and *Drosophila* embryos (Wang et al., 1980). The reduced denatured protein is a single polypeptide chain of M_r 100K (HeLa), 111K (wheat germ), or 110K (*Drosophila*). In one of these cases (Liu & Miller, 1981), it has been shown that prevention of proteolysis during isolation and purification of topoisomerase accounts for the finding of higher molecular weight protein. We cannot con-

† From the Department of Cell and Tumor Biology, Roswell Park Memorial Institute, Buffalo, New York 14263, and the Department of Biochemistry, Roswell Park Graduate Division, State University of New York, Buffalo, New York 14263. *Received November 1, 1982.* This research was supported by National Institutes of Health Grant CA-23996 and National Science Foundation Grant PCM-7823757.

* Address correspondence to this author at the Department of Cell and Tumor Biology, Roswell Park Memorial Institute.
‡ Present address: Department of Human Genetics, Roswell Park Memorial Institute, Buffalo, NY 14263.

[1] Abbreviations: M_r, relative molecular weight; $NaDodSO_4$, sodium dodecyl sulfate; PMSF, phenylmethanesulfonyl fluoride; Tris, tris(hydroxymethyl)aminomethane; EDTA, ethylenediaminetetraacetic acid; Hepes, *N*-(2-hydroxyethyl)piperzine-*N'*-2-ethanesulfonic acid.

0006-2960/83/0422-2025$01.50/0